

Molecular Dynamics Study of the Molecular Weight Dependence of Surface Tensions of Normal Alkanes and Methyl Methacrylate Oligomers

Chunli Li and Phillip Choi*

Department of Chemical and Materials Engineering, University of Alberta,
Edmonton, Alberta, Canada T6G 2G6

Received: October 27, 2005; In Final Form: February 6, 2006

Surface tensions (γ) of normal alkanes and methyl methacrylate (MMA) oligomers at various molecular weights in the low molecular weight range were computed using a newly proposed molecular dynamics (MD) simulation strategy which was developed based on the definition of $\gamma = (\partial U / \partial \sigma)_{n,V,S}$. The MD simulations, even with the use of a generic force field, reproduced the experimentally observed molecular weight dependence of γ (i.e., $\gamma \propto M_n^{-2/3}$, where M_n is the number-average molecular weight) for both series of oligomers. Analysis of the data reveals that solvent accessible surface area, one of the key input variables used for the calculation of γ , exhibits an $M_n^{2/3}$ (rather than M_n^1) dependence. The reason for such dependence is that solvent accessible surface area formed by the chainlike small molecules depends, to a larger extent, on their orientations rather than their size. However, this is not the case for high molecular weight molecules as solvent accessible surface area of such surfaces are determined by the orientations of their segments which are determined by the conformations of the molecules. This may explain why surface tension of polymers experimentally exhibits an M_n^{-1} dependence. It is inferred that the corresponding molecular weight dependence of the entropy changes associated with molecules in the low and high molecular weight ranges would be different.

1. Introduction

Inasmuch as the concept of surface tension is relevant to a variety of physical phenomena and engineering applications, there exists a wealth of information about it in the literature. In particular, Dee and Sauer have done an extensive review on numerous theoretical and experimental studies of the surface tension of polymers over a wide range of molecular weights.¹ As mentioned in their review article, it has long been observed that surface tension (γ) exhibits an $M_n^{-2/3}$ dependence (where M_n is the number-average molecular weight) for low molecular weight polymers (i.e., oligomers),² and recent experimental studies show that the surface tension of polymer melts with moderate to high molecular weights actually exhibits an M_n^{-1} dependence.³

Over the past two decades, molecular simulation techniques have also been developed to compute surface tension. Three types of simulation techniques are available, and they are discussed in detail in a review article written by Gloor et al.⁴ Within the context of such techniques, these general approaches are referred to as the mechanical approach,⁵ thermodynamic approach,^{4,6} and finite-size scaling concept based approach.^{7,8} Since our proposed method follows the thermodynamic approach and our simulation results will be compared with those obtained from the more popular mechanical approach, we will only provide the basic ideas involved in the first two simulation approaches here. The reader is referred to refs 7 and 8 for the details of the finite-size scaling method. The mechanical approach uses the distribution function method in which the tangential component of the pressure tensors ($P_t(z)$) of the molecules in the interfacial region bound by the coordinates z_α and z_β in the normal direction of the interface of a model system

is used to calculate surface tension. This is based upon the classical equation developed by Kirkwood and Buff in 1949⁵

$$\gamma = \int_{z_\alpha}^{z_\beta} [P - P_t(z)] dz \quad (1)$$

where γ is the surface tension and P is the uniform normal pressure of the model system. This equation essentially provides the link between the intermolecular forces experienced by the molecules in the interfacial region and surface tension measured macroscopically. However, since most of the generic force fields used in molecular simulation cannot reproduce pressure tensors very well,⁹ use of such an approach, especially for chainlike molecules, would lead to inaccurate prediction of surface tension.

The thermodynamic approach is also frequently used to calculate surface tension. One way to implement such an approach is to calculate the internal energy change upon creation of surfaces to a bulk model system (i.e., $(\partial U / \partial \sigma)_{n,V,T}$) and combine it with the experimental information about the corresponding entropy change (i.e., $T(\partial S / \partial \sigma)_{n,V,T}$) to obtain surface tension. This is because the entropy term cannot be evaluated directly from molecular simulation. The approach is based on the most common definition of surface tension as shown in the following equation

$$\gamma = \left(\frac{\partial A}{\partial \sigma} \right)_{n,V,T} = \left(\frac{\partial U}{\partial \sigma} \right)_{n,V,T} - T \left(\frac{\partial S}{\partial \sigma} \right)_{n,V,T} \quad (2)$$

where γ is the surface tension of the model system, A is the Helmholtz free energy of the system, and σ is the area of the surface that separates the bulk liquid phase and its equilibrium vapor phase. U and S are the internal energy and entropy of the system. The subscripts n , V , and T denote the number of molecules, total volume, and temperature of the system. In

* To whom correspondence should be addressed.

particular, Mansfield and Theodorou demonstrated that reasonably accurate $(\partial U/\partial \sigma)_{n,V,T}$ values could be obtained by calculating the internal energy difference between a thin film model and a bulk liquid model with the same number of molecules at the same temperature.¹⁰ In their approach, the thin film model was generated by imposing two well-defined surfaces which were located at the upper and lower extremes of the bulk cell and normal to the z axis. $(\partial U/\partial \sigma)_{n,V,T}$ is simply calculated using the following expression

$$\left(\frac{\partial U}{\partial \sigma}\right)_{n,V,T} = \frac{\langle U_{2D} \rangle - \langle U_{3D} \rangle}{\sigma} \quad (3)$$

where σ denotes the total surface area of the two surfaces created on both sides of the bulk cell (i.e., $2 L_x L_y$). Here, L_x and L_y are the dimensions of the thin film in the x and y directions (z being the direction normal to the film surface). $\langle U_{2D} \rangle$ and $\langle U_{3D} \rangle$ represent the average internal energy of the model system in the thin film and bulk states, and such quantities are calculated from the corresponding molecular dynamics (MD) simulations at the same T . However, V has changed considerably in the process. This is because such an equilibrated thin film structure would contain two interfacial regions that have a higher volume per unit mass than the bulk region of the system. Therefore, the total volume occupied by the same number of molecules in the thin film model would be larger than the volume of the 3D periodic bulk model. Obviously, this is not an issue for a macroscopic system because the volume of the interfacial region is much smaller than the total volume of the system. In addition, the total volume of such a small thin film model is difficult to define as its surfaces are fairly rough. In our view, it is more appropriate to define the area using the concept of solvent accessible surface area (see the discussion below) and use it to define the total volume of the thin film model.¹¹

Nonetheless, Mansfield and Theodorou were able to reproduce the experimental data even with the use of a surface area of $2L_x L_y$ and showed that the entropy term in eq 2 is not negligible. The latter finding is somewhat expected as surface tensions of polymer melts are generally measured at relatively high temperatures (e.g., 400 K). Unless the entropy term is extremely small, say on the order of 10^{-4} mJ/(m² K), it would lead to erroneous predictions when the entropy term is neglected. However, it is worth noting that Mattice and co-workers used a different method and found that reasonable predictions of surface tensions of polymer melts, such as poly(1,4-*cis*-butadiene),¹² polyethylene,¹³ polybenzoxazine,¹⁴ etc., could be obtained by ignoring the entropy term in eq 2. The method by which the authors used to create surfaces is to elongate the three-dimensional periodic liquid model cell in one direction up to a point that the parent chains in the periodic simulation cell do not sense the existence of their periodic images in the elongating direction (see Figure 1).

In view of the difficulty associated with the second approach, we propose here a new approach to compute γ using a less popular definition of surface tension as shown in the following equation:¹⁵

$$\gamma = \left(\frac{\partial U}{\partial \sigma}\right)_{n,V,S} \quad (4)$$

Obviously, use of the definition shown in eq 4 suffers from the volume and surface area issues mentioned above as well. But it provides the basis for the direct calculation of surface tension without the need to evaluate the entropy term as S is supposed to be fixed. The key issue here is how to keep S constant. In

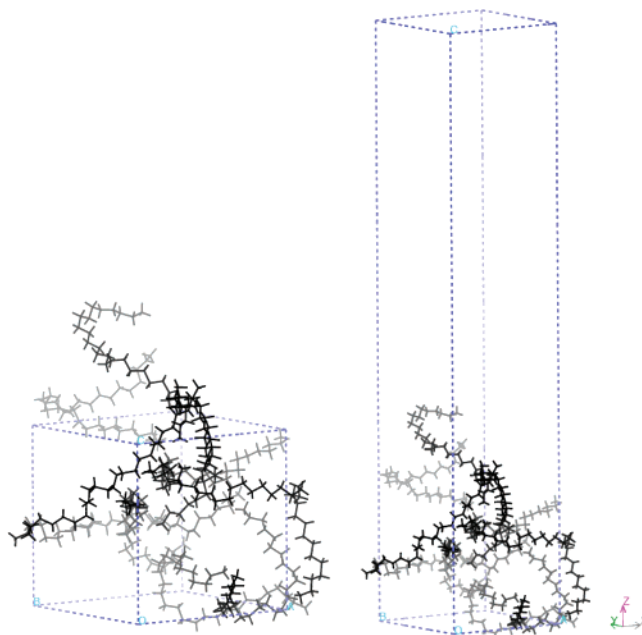


Figure 1. Image of normal alkane chain models (left, three-dimensional periodic liquid model; right, thin film model).

this regard, we adopted an approach similar to a procedure that is commonly used in the calculation of cohesive energy density (CED) for such a purpose.^{16,17} In particular, the configuration of the molecules used in the thin film and bulk liquid models is fixed to maintain constant entropy. To test the validity of the new strategy, we applied it to two fairly different series of low molecular weight compounds—normal alkanes and methyl methacrylate (MMA) oligomers—to check if we could reproduce their surface tension values and the corresponding experimentally observed molecular weight dependence. The choices of the oligomers were made simply because of the availability of surface tension data and the fact that molecules of respective oligomers interact with each other through different types of intermolecular forces.¹⁸ Finally, it should be pointed out that our proposed method is similar to the test area method recently proposed by Gloor et al.⁴

2. Molecular Dynamics Simulation

2.1. Simulation Details. All simulations were carried out on a Silicon Graphics (SGI) workstation cluster along with the use of commercial software—Cerius2 version 4.0 purchased from Accelrys. A generic force field DREIDING 2.21 developed by Mayo et al. was used for both series of oligomers which were represented by explicit atomistic models.¹⁹ However, for the alkane models, instead of using the default Lennard-Jones (LJ) parameters for carbon–carbon interactions, the LJ parameters of Ryckaert and Bellemans were used as such parameters yield satisfactory estimation of cohesive energy density for low molecular weight alkanes as demonstrated previously.²⁰ The choice of the force field and LJ parameters was based on the balance of the availability of computational resources and accuracy of the results. For the normal alkane models, zero charges were assigned, while the charge equilibration method²¹ was used to determine the partial atomic charges for all atoms made up of the MMA oligomers. For each series of oligomers, five models with chain lengths ranging from about 10 to 200 backbone carbons, which cover the so-called low molecular weight ranges as defined experimentally, were used. Multiple chain models were used for simulating the condensed phase of

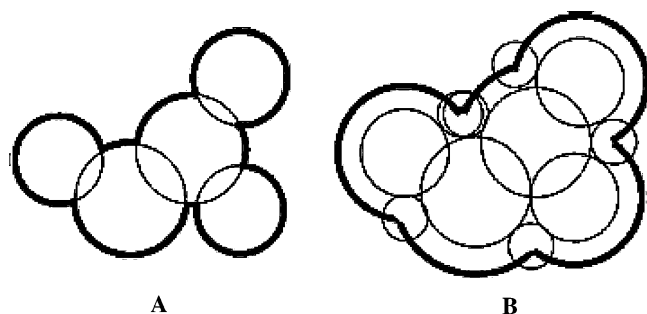


Figure 2. Molecular surface models: (A) van der Waals surface; (B) solvent accessible surface.

TABLE 1: Characteristics of the Normal Alkane Models with Chain Lengths from 13 to 200 Carbons

| models | molecular weight (g/mol) | density (g/cm ³) | no. of chains for calculation | cell side length (Å) |
|--------|-----------------------------|---------------------------------|----------------------------------|-------------------------|
| PEC13 | 184.4 | 0.6604 | 10 | 16.67 |
| PEC20 | 282.6 | 0.7009 | 10 | 18.85 |
| PEC30 | 422.9 | 0.7276 | 10 | 21.30 |
| PEC60 | 843.6 | 0.7533 | 4 | 19.52 |
| PEC200 | 2807 | 0.7706 | 1 | 18.22 |

TABLE 2: Characteristics of the MMA Oligomers Models with Chain Lengths from 10 to 200 Repeat Units

| models | molecular weight (g/mol) | density (g/cm ³) | cell side length (Å) |
|----------|-----------------------------|---------------------------------|-------------------------|
| PMMA 10 | 1003 | 1.11 | 11.45 |
| PMMA 30 | 3006 | 1.11 | 16.51 |
| PMMA 50 | 5008 | 1.11 | 19.57 |
| PMMA 100 | 10014 | 1.11 | 24.66 |
| PMMA 200 | 20026 | 1.11 | 31.06 |

the normal alkanes except the model with 200 backbone carbons. However, single-chain models were used for MMA oligomers as their chain architecture is much more complex than that of normal alkanes. Characteristics of the above-described models are presented in Tables 1 and 2. The experimental bulk densities at the simulation temperatures (150 °C for normal alkanes and 180 °C for MMA oligomers) and the corresponding cubic simulation cell sizes are also given in the same tables.²² For the MMA oligomers, owing to the lack of experimental density data on the oligomers at various chain lengths, density of PMMA at 180 °C was used for all models.

The initial liquid-state models of the oligomers were built using the method of Theodorou and Suter along with their experimental density values.²³ Each initial three-dimensional periodic simulation cell, after energy minimization, was subjected to a 1000 K MD annealing for a period of 100 ps before the low-temperature MD simulations at the corresponding simulation temperatures (150 °C for normal alkanes and 180 °C for MMA oligomers) were carried out. The simulation time was set at 1 ns, and the time step used was 1 fs. Ten snapshots of the last 100 ps, recorded every ps, of the 1 ns simulation were used for the calculation of the potential energy of the liquid-state model, denoted as U_{3D} , respectively. For each of such snapshots, the z direction of the 3D periodic simulation cell was elongated until it was long enough that no interactions between neighboring periodic cells in the z direction could be found (see Figure 1), and the corresponding U_{2D} was calculated. The total volume of the thin film model was determined based on the volume bounded by the two solvent accessible surfaces (see Figure 2 and the discussion about solvent accessible surface area below). Here, a series of hard spherical probes with different radii were used to identify the area that would yield the total volume which was equal to that of the original 3D

model. The average total volume of the thin film model was also calculated by averaging the total volumes of the last 100 snapshots.

In this way, all subscript variables appearing in eq 4 (i.e., n , V , and S) are kept constant. It should be emphasized that $\langle U_{2D} \rangle$ which appears in eq 3 does not require the entropy (i.e., conformations of the molecules) to be fixed. Therefore, equilibrated structures of the thin film model should be used. However, when eq 4 is used, $\langle U_{2D} \rangle$ should be calculated using the same conformations of the molecules from the 3D periodic simulation cell but with interactions in the z direction removed. This procedure is essentially identical to a well-accepted procedure used for the calculation of the cohesive energy density of chain molecules in which the potential energy of the molecules in an ideal gas state is calculated using the same conformation of the molecules obtained from the bulk cell but with all three-dimensional periodic boundary conditions removed.²⁴ It should be emphasized that the thin film models we generate to calculate $\langle U_{2D} \rangle$ do not have a temperature associated with them as they are merely copies of the configurations of the molecules of the MD trajectories of the bulk state model (no kinetic energy). The temperature that is associated with the computed surface tension corresponds to the one used for the bulk state model.

2.2. Surface Area. As mentioned, use of the flat surface areas (i.e., $2L_xL_y$) as σ shown in eq 3 for the thin film models with thicknesses in the length scale of few nanometers (either the equilibrated or nonequilibrated one) is not appropriate as surfaces of such models are “rough”. In our view, such “rough” surfaces are better described by the concept of solvent accessible surface area.¹¹ Solvent accessible surface area is generated by the center of a solvent molecule probe (modeled as a rigid sphere) when it is being “rolled” over the van der Waals surface of the model molecules as depicted in Figure 2. Obviously, different surface areas would be obtained using probes with different radii. Therefore, specifying the radius of the spherical probe for such a “rolling” process is critical. In this regard, we tested a series of probes with radii ranging from 0.5 to 3.5 Å, and the solvent accessible surface area that would yield a total volume that is equal to volume of the liquid-state model would be used in the calculation of γ . Owing to the time-consuming nature of such calculations, only 10 snapshots of the last 100 ps of each MD simulation were obtained and used for calculating the average.

3. Results and Discussion

The probe size dependence of the solvent accessible surface area and the corresponding total volume of the thin film models of the normal alkane with 30 backbone carbon atoms and MMA oligomer with 30 repeating units are shown in Figures 3 and 4, respectively. Similar results for the two oligomers at various chain lengths are omitted for clarity. As can be seen, the solvent accessible surface area decreases with increasing probe size while the total volume of the thin film bounded by the solvent accessible surfaces exhibits an opposite trend. The first observation is simply attributed to the fact that larger probes would not be able to detect the detailed contour of the surfaces. As a result, the solvent accessible surface area and its roughness would decrease. Hence, the total volume enclosed by the solvent accessible surfaces would include a considerable amount of free volumes leading to a larger total volume. As mentioned, to determine the area that should be used in the calculation of surface tension, we chose the solvent accessible surface area that would yield a total volume which was equal to the volume

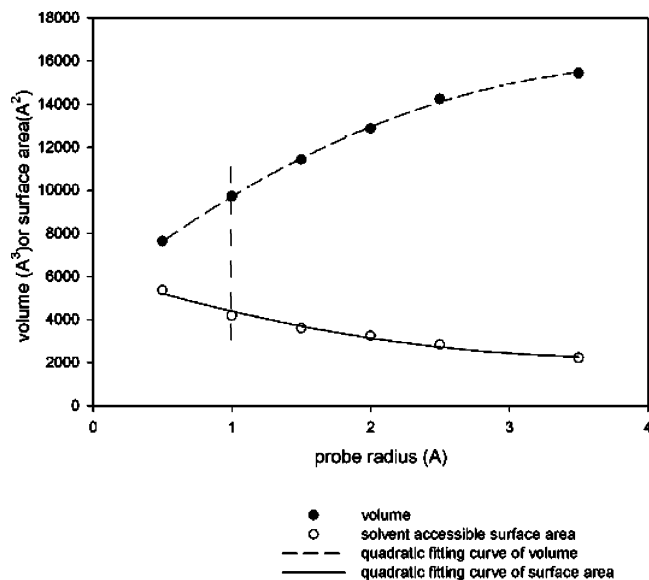


Figure 3. Probe size dependence of solvent accessible surface area and the corresponding total volume of the thin film models for the normal alkane chains with 30 carbon atoms (the probe size marked by the dashed line corresponds to the one used in this paper).

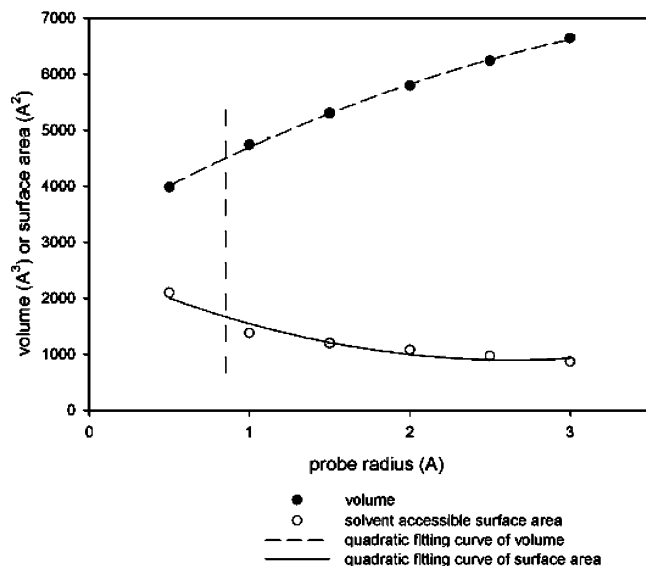


Figure 4. Probe size dependence of solvent accessible surface area and the corresponding total volume of the thin film models for the MMA oligomer with 30 repeating units (the probe size marked by the dashed line corresponds to the one used in this paper).

of the 3D periodic simulation cell from which the thin film model was generated. It should be noted again that the molecules in the thin film model possess the same conformation as those in the 3D periodic simulation cell. Consequently, the energy difference between the thin film and liquid-state models is purely attributed to the internal energy change due to the difference in the intermolecular interactions (not from the change in the bonded energy). The respective simulation results, plotted against $M_n^{-2/3}$ for the normal alkanes and MMA oligomers, are shown in Figures 5 and 6 along with the corresponding experimental results. It is obvious in both cases that the computed data points are highly linear, indicating that the surface tension of these two chemically different oligomers exhibit the expected $M_n^{-2/3}$ dependence. Using slopes of the regression lines obtained for the experimental surface tension data (no error bars) as references,^{9,19,20,22} we consider the slopes we obtained to be in good agreement with experiment, especially in the case of

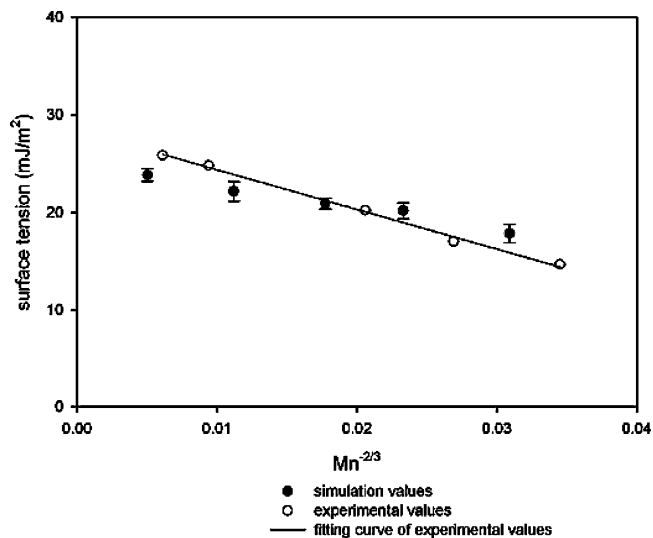


Figure 5. Molecular weight dependence of surface tension for normal alkanes obtained from our simulations (solid circles) compared with experimental data (open circles) (ref 18).

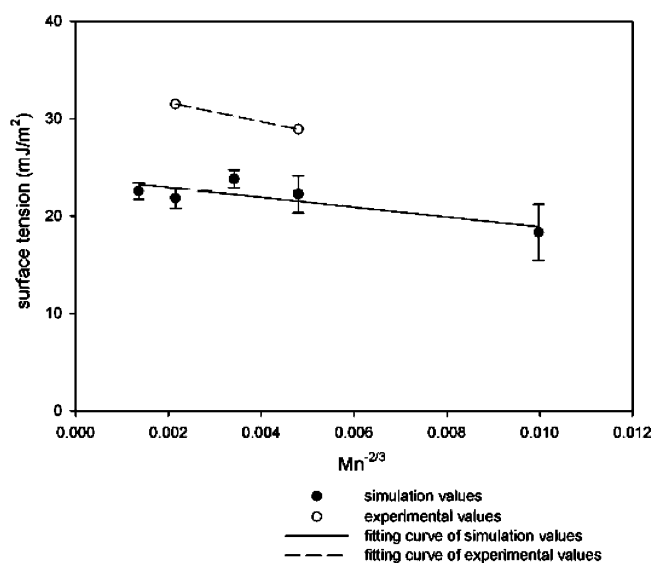


Figure 6. Molecular weight dependence of surface tension for MMA oligomers obtained from our simulations (solid circles) compared with experimental data (open circles) (refs 27–29).

MMA oligomers (there are only two experimental data points available for the MMA oligomers). Nonetheless, the experimental and our simulation results indicate that the $M_n^{-2/3}$ dependence of surface tension is universal but the proportional constant (i.e., the slope) depends on the chemical characteristics of the oligomer. It is worth noting that Nicolas and Smit have done MD simulations to calculate surface tensions of three linear alkanes (C6, C10, and C16) by employing the mechanical approach with the use of OPLS and SKS force fields.^{25,26} Since sizes of the alkanes and simulation temperatures used by these authors are quite different from what we used, no direct comparison is made here. Nevertheless, the computed γ of the three alkanes that Nicolas and Smit used are ~ 6 mJ/m² (SKS model for C6 at 450 K), ~ 9 mJ/m² (SKS model for C10 at 450 K), and ~ 18 mJ/m² (SKS model for C16 at 380 K) which are significantly lower than the experimental values ($\sim 15\%$).

Compared with normal alkanes, it is clear that the numerical values of the computed surface tension of MMA oligomers deviate significantly from experiment. This is simply because DRIEDING 2.21 is not optimized for MMA oligomers. How-

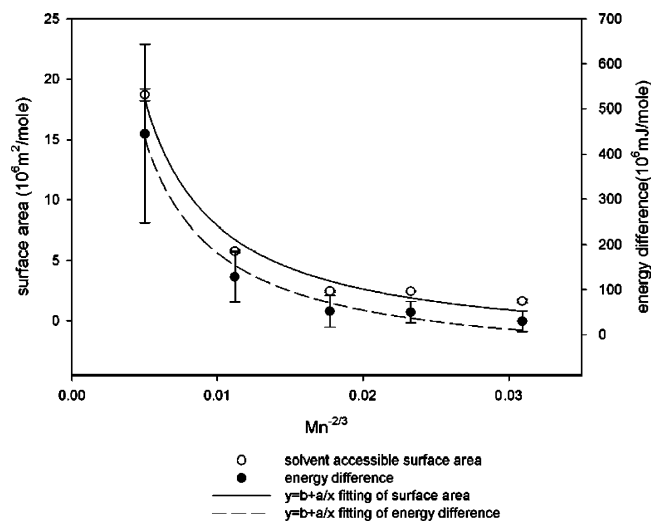


Figure 7. Molecular weight dependence of surface tension components for normal alkanes, with solvent accessible surface area (open circles) labeling on the left vertical axis and energy difference ($\langle U_{2D} - U_{3D} \rangle$) (solid circles) labeling on the right vertical axis. The surface tension data shown in Figure 5 were obtained by dividing ($\langle U_{2D} - U_{3D} \rangle$) by the solvent accessible surface area.

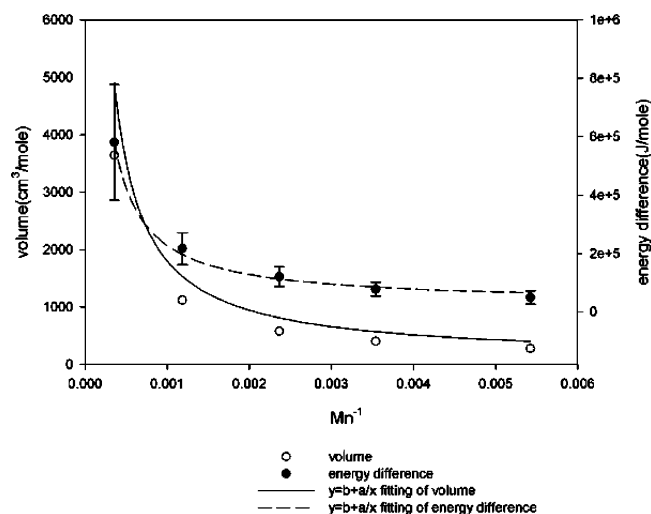


Figure 8. Molecular weight dependence of cohesive energy density components for normal alkanes, with molar volume (open circles) labeling on the left vertical axis and energy difference ($\langle U_{vac} - U_{3D} \rangle$) (solid circles) labeling on the right vertical axis.

ever, it is interesting to note that the newly proposed molecular simulation procedure, even with the use of a generic force field, yielded the molecular weight dependence of the surface tension ($M_n^{-2/3}$) quite well for the two drastically different oligomers. In other words, our models implicitly captured the physics involved. To this end, we further analyze both the surface tension and CED data to identify the root cause for the observed behavior.

Figure 7 shows the molecular weight dependence of $\langle U_{2D} - U_{3D} \rangle$ and of the corresponding solvent accessible surface area for the normal alkanes, while Figure 8 is for $\langle U_{vac} - U_{3D} \rangle$ and molar volume for the same set of models. The corresponding trends for the MMA oligomers are omitted as a similar trend was observed. It should be noted that the molar volumes shown in Figure 8 are from experiment while all other data points in Figures 7 and 8 were obtained from our MD simulations. It is interesting to observe that molecular weight dependence of the solvent accessible surface area and the associated $\langle U_{2D} - U_{3D} \rangle$ as well as of the molar volume and $\langle U_{vac} - U_{3D} \rangle$ resemble each

other when they were plotted against $M_n^{-2/3}$ and M_n^{-1} , respectively. In particular, the molar volume shows an inverse dependence of M_n^{-1} , while the solvent accessible surface area also shows an inverse dependence but on $M_n^{-2/3}$. The inverse dependence of M_n^{-1} for the molar volume and the associated $\langle E_{vac} - E_{3D} \rangle$ simply means that both quantities are linearly proportional to the average size of the molecules. The former dependence is expected based upon the definition of molar volume. The latter also seems reasonable as the vaporization process involves the elimination of the intermolecular forces experienced by the molecules in the three-dimensional space which should vary linearly with the average size of the molecules. And such dependence should not change as the size of the molecules becomes larger and is applicable to the whole molecular weight range as observed experimentally.

Regarding the solvent accessible surface area, our simulation results show that it depends, to a less extent, on the size of the oligomers, only to the power of $2/3$ (i.e., $1/M_n^{-2/3}$) rather than 1. The corresponding $\langle U_{2D} - U_{3D} \rangle$ also exhibits a similar functional dependence. Consequently, when both quantities were combined, that led to an $M_n^{-2/3}$ dependence of surface tension. Since high molecular weight normal alkanes ($M_n > 500 \text{ g/mol}$) exhibit an M_n^{-1} dependence of surface tension (experimental observation),¹⁸ it is conjectured that the exponent of the molecular weight dependence of the solvent accessible surface area for high molecular weight normal alkanes may have a value of 1. If that is the case, what is required to be explained is why low molecular weight normal alkanes exhibit an $M_n^{2/3}$ dependence on the solvent accessible surface area (therefore surface tension) while high molecular weight ones exhibit an M_n^{-1} dependence. Considering the manner by which solvent accessible surface areas were evaluated in the present work, it seems that the higher the molecular weight of the oligomer is, the rougher the surface is. Figures 9 and 10, which show the solvent accessible surfaces for the lowest and highest molecular weight normal alkane and MMA oligomers used, are used to illustrate such observation. In other words, the molecular weight dependence of the solvent accessible surface area seems to be related to the roughness of the nonequilibrium surfaces created by the elongation process. In particular, it was observed that surfaces of the oligomers with 200 backbone carbons tend to exhibit more chain bending that leads to rougher surfaces. For low molecular weight oligomers, roughness seems to be related to the orientations of the molecules (no chain bending) rather than their size. One can imagine that in the extreme case, when all such small molecules line up in the direction normal to the surface, the roughness of the surface would be a weak function of the size of the molecules. On the other hand, when all molecules lie in the plane of the surface, the surface accessible surface area covered by the molecules would depend, to a larger extent, on the size of the molecules. However, since all of these molecules orient randomly, the exponent of the molecular weight dependence of the solvent accessible surface area should be expected to be less than 1. We believe the observed exponent of $2/3$ could probably be derived mathematically based upon the orientations of the molecules and the radius of the probe used. Since the critical molecular weight above which normal alkanes start to chain fold in vacuum is about 500 g/mol, it is speculated that above such a molecular weight, the roughness of the surfaces of normal alkanes would depend on the orientations of the segments exposed to the surface, which would depend on the chain length of the molecules. It should be pointed

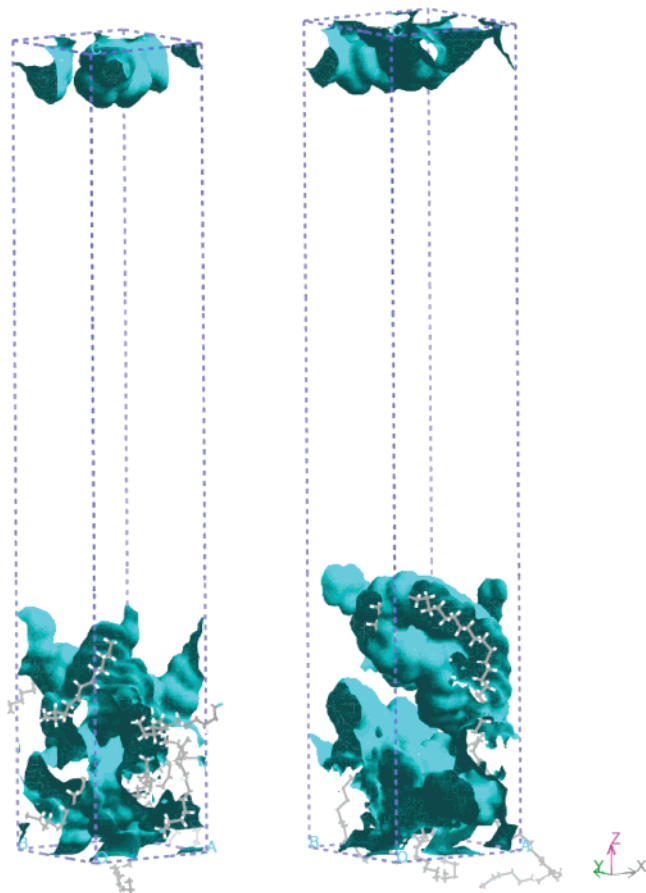


Figure 9. Solvent accessible surfaces of normal alkane models (left, PEC13; right, PEC200).

out that the chain segments of the high molecular weight molecules would orient themselves more or less in a random fashion.

Two points are noteworthy. First, it should be pointed out that the above discussion is based on the nonequilibrium surfaces created by the elongation process; the orientations and/or conformations of the molecules are identical to those in their corresponding bulk state. The conformations of the molecules correspond to a hypothetical state of the systems that we created to evaluate surface tension in accordance with the surface tension definition shown in eq 4. In reality, those surfaces would not be as rough as shown in Figures 9 and 10 as the surface molecules would move closer to each other to form the interfacial region at a density value lower than that of the bulk to minimize the interaction with the vacuum. Second, our proposed procedure may allow us to calculate $(\partial S/\partial \sigma)_{n,V,T}$ directly (note that $(\partial S/\partial \sigma)_{n,V,T} = d\gamma/dT$) as we can compute γ , at least in principle, at different temperatures. However, as Dee and Sauer pointed out in their review article,¹⁸ the temperature dependence of surface tension (i.e., $d\gamma/dT$) for a variety of oligomers and polymers is on the order of magnitude of -0.05 mJ/m² K. In particular, the experimental value of $d\gamma/dT$ for C11 is -0.097 mJ/m² K.³ The lowest molecular weight alkane that we used was C13, and the corresponding computed γ carries an uncertainty of ± 0.94 mJ/m² K (one standard deviation). Obviously, the error associated with the computed γ is about 1–2 orders of magnitude larger than the expected value of $d\gamma/dT$, making an accurate estimation of $d\gamma/dT$ rather difficult. Nonetheless, our preliminary results on C20 over a temperature range of 10 K show qualitatively that γ is fairly insensitive to temperature which confirms the validity of our procedure.

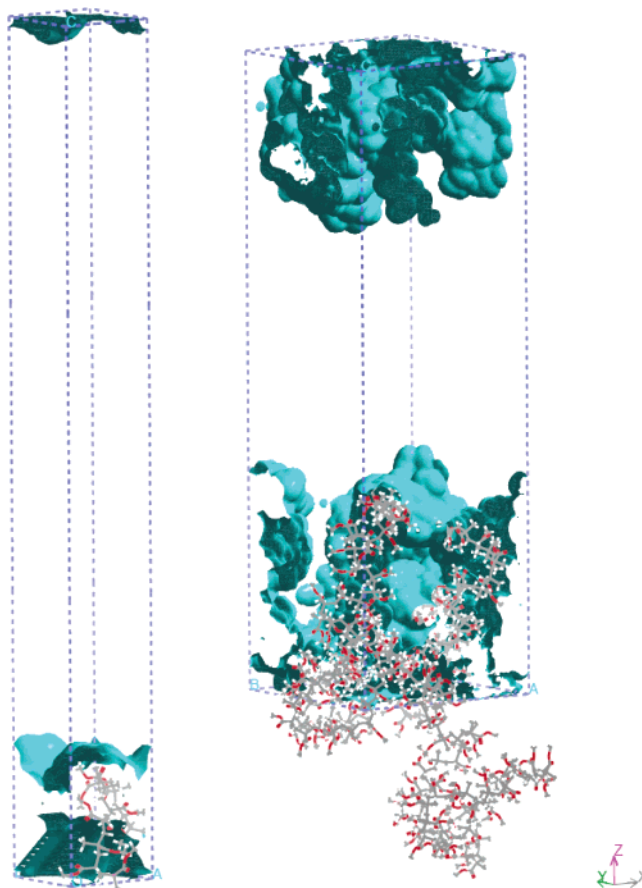


Figure 10. Solvent accessible surfaces of MMA oligomer chains (left, PMMA10; right, PMMA200).

However, since quantitative agreement was not reached, we decided not to include such results in the current manuscript. More MD runs are required for each temperature to reduce the errors associated with γ and therefore to have a more reliable estimation of $d\gamma/dT$. This is practically infeasible to us at this point. However, we will be performing such calculations and report the results in due course as more computer resources become available since our proposed procedure may provide us with a direct route to accurately calculate $(\partial S/\partial \sigma)_{n,V,T}$ (note that $d\gamma/dT = (\partial S/\partial \sigma)_{n,V,T}$). This means that we can calculate γ directly using eq 2 along with our method for the calculation of $(\partial S/\partial \sigma)_{n,V,T}$ and the method of Mansfield and Theodorou for $(\partial U/\partial \sigma)_{n,V,T}$. Obviously, such an approach would require much more effort than our proposed method to calculate γ .

4. Conclusions

A novel molecular dynamics simulation procedure, based upon a less common definition of surface tension, has been proposed to compute the surface tension of oligomers. In particular, the new procedure was tested on normal alkanes and MMA oligomers. It was found that the deviation of the surface tension for MMA oligomers is very likely attributed to the generic nature of the force field used. Nonetheless, the new method is able to yield the molecular weight dependence of these two vastly different series of oligomers. Simulation results are in good agreement with the experimental observation of $M_n^{-2/3}$ dependence of surface tension. Analysis of the data revealed that it may originate from the fact the roughness of the surface determines such molecular weight dependence. In particular, for molecules in the low molecular weight range, roughness of their surfaces depends on the orientations of the

molecules and to a less extent to the size of the molecules. However, in the high molecular weight range, surface roughness would likely depend on the orientations of the segments (i.e., conformation) made up of the molecules in the interfacial region, therefore on the size of the molecules.

Acknowledgment. Funding from the Natural Science and Engineering Research Council of Canada is gratefully acknowledged. This research has been enabled by the use of WestGrid computing resources, which are funded in part by the Canada Foundation for Innovation, Alberta Innovation and Science, BC Advanced Education, and the participating research institutions. WestGrid equipment is provided by IBM, Hewlett-Packard, and SGI. Finally, the authors thank Drs. Janet Elliot and Zhenghe Xu for many stimulating discussions.

References and Notes

- (1) Dee, G. T.; Sauer, B. B. *J. Colloid Interface Sci.* **1992**, *152*, 86.
- (2) Roe, R. J. *Proc. Natl. Acad. Sci. U.S.A.* **1966**, *56*, 819.
- (3) Sauer, B. B.; Dee, G. T. *Macromolecules* **1991**, *24*, 2124.
- (4) Gloor, G. J.; Jackson, G.; Blas, F. J.; de Miguel, E. *J. Chem. Phys.* **2005**, *123*, 134703.
- (5) Kirkwood, J. E.; Buff, F. P. *J. Chem. Phys.* **1949**, *17*, 338.
- (6) Bennett, C. H. *J. Comput. Phys.* **1976**, *22*, 245.
- (7) Binder, K. *Phys. Rev. A* **1982**, *25*, 1699.
- (8) Buff, F. P.; Lovett, R. A.; Stillinger, F. H., Jr. *Phys. Rev. Lett.* **1965**, *15*, 621.
- (9) Choi, P. *Polymer* **2000**, *41*, 8741.
- (10) Mansfield, K. F.; Theodorou, D. N. *Macromolecules* **1990**, *23*, 4430.
- (11) Connolly, M. L. *J. Am. Chem. Soc.* **1985**, *107*, 1118.
- (12) He, D.; Reneker, D. H.; Mattice, W. L. *Comput. Theor. Polym. Sci.* **1997**, *1*, 19.
- (13) Misra, S.; Fleming, P. D., III; Mattice, W. L. *J. Comput.-Aided Mater. Des.* **1995**, *2*, 101.
- (14) Kim, W. K.; Mattice, W. L. *Langmuir* **1998**, *14*, 6588.
- (15) Becher, P. *Encycl. Emulsion Technol.* **1983**, 17.
- (16) Zhao, L.; Choi, P. *J. Chem. Phys.* **2004**, *120*, 1935.
- (17) Maranas, J. K.; Mondello, M.; Grest, G. S.; Kumar, S. K.; Debenedetti, P. G.; Graessley, W. W. *Macromolecules* **1998**, *32*, 6991.
- (18) Dee, G. T.; Sauer, B. B. *Adv. Phys.* **1998**, *2*, 161.
- (19) Mayo, S. L.; Olafson, B. D.; Goddard, W. A., III. *J. Phys. Chem.* **1990**, *94*, 8897.
- (20) Rychaert, J. P.; Bellemans, A. *Chem. Phys. Lett.* **1975**, *30*, 123.
- (21) Rappe, A. K.; Goddard, W. A. *J. Phys. Chem.* **1991**, *95*, 3358.
- (22) Doolittle, A. K. *J. Chem. Eng. Data* **1964**, *2*, 275.
- (23) Theodorou, D. N.; Suter, U. V. *Macromolecules* **1985**, *18*, 1467.
- (24) Rodgers, P. A. *J. Appl. Polym. Sci.* **1993**, *48*, 1061.
- (25) Nicolas, J. P.; Smit, B. *Mol. Phys.* **2002**, *100*, 2471.
- (26) Jorgensen, W. L.; Madura, J. D.; Swenson, C. J. *J. Am. Chem. Soc.* **1984**, *106*, 6638.
- (27) Goudeau, S.; Galy, J.; Gerard, J. F.; Gulchiron, R.; Barrat, J. L. *Mater. Res. Soc. Symp.* **2000**, FF9.2.1.
- (28) Wu, S. *Polymer Interface and Adhesion*; Marcel Dekker: New York, 1982; p 88.
- (29) Wu, S. *J. Phys. Chem.* **1970**, *74*, 632.